States in ^{243}Pu from the (n,γ), (d,p), and (d,t) reactions*

R. F. Casten and W. R. Kane
Brookhaven National Laboratory, Upton, New York 11973

J. R. Erskine, A. M. Friedman, and D. S. Gale†
Argonne National Laboratory, Argonne, Illinois 60439

(Received 26 February 1976)

The levels of ^{243}Pu have been studied with the ^{242}Pu$(n,\gamma)^{243}$Pu, ^{242}Pu$(d,p)^{243}$Pu, and ^{244}Pu$(d,t)^{243}$Pu reactions. Nearly all levels detected below 1100 keV have been assigned to rotational bands built upon Nilsson orbitals by considering the expected rotational spacings, the (d,p) and (d,t) cross sections which are characteristic of the specific orbital, the spin-parity information deduced from the (n,γ) data, and the systematics of nearby nuclei. In all, 12 rotational bands were identified. In addition a likely octupole excitation was located at 704 keV. Of particular interest is the fact that the $1/2^-[501]$ orbital is not significantly fragmented in ^{243}Pu. Nilsson model and Coriolis calculations are performed and the predictions for γ-ray transition rates are compared to the empirical results. In general good agreement is found, but with a few noted exceptions.

[NUCLEAR REACTIONS ^{242}Pu(n,γ), $E=2.96$ eV; measured E_γ, I_γ, γ-γ coin. ^{243}Pu deduced levels, J, π, Ge(Li) detector. ^{242}Pu(d,p), ^{244}Pu(d,t), $E=12$ MeV; measured Q_0, E_x, and $\sigma(\theta)$. ^{243}Pu deduced levels, l. Enriched targets. ^{243}Pu deduced levels, J, π, Nilsson assignments, rotational bands from combined experiments. Calculated γ-ray transition probabilities with Nilsson model and Coriolis interaction.]

I. INTRODUCTION

In recent years there has been considerable interest in developing the level schemes of the actinide nuclei. Detailed studies of odd mass nuclei in this region can provide critical information on the locations of Nilsson orbitals and their energy systematics. Theoretically these depend on the quadrupole as well as higher multipole moments of the nuclear shape and therefore provide access to information by a means complementary to Coulomb excitation and α particle scattering. Furthermore, the Nilsson energies in this mass region are important in calculations relating to vibrational excitations, (p,t) and (t,p) cross sections to 0^+ states in even-even actinide nuclei and, to some extent, for predictions of fission barriers and the stability of heavy nuclei.

Experimentally there are certain difficulties inherent in this mass region but a large number of charged-particle reactions have nevertheless been carried out.[1-5] Some studies of the (n,γ) reaction and radioactive decay have also been done.[5-8] A frequent problem with the (n,γ) reaction, however, is a relatively low thermal radiative neutron-capture cross section: specifically, the ratio of that cross section relative to neutron-induced fission cross sections. Often, too, γ decay of the active target provides a source of contaminant γ-ray lines. Thus, the resonant (n,γ) reaction is an extremely useful tool in those cases where a given resonance has a large cross section and, in particular, a large ratio of capture to fission widths.

The ^{242}Pu(n,γ) reaction provides such a case since the 2.66 eV resonance has a cross section of 65 000 b compared to 18 b for thermal capture.[9] The fission width is negligible for this resonance as well. The large resonance cross section also permits the use of relatively small amounts of ^{242}Pu target material, thereby reducing both the background decay γ-ray activity and the γ-ray self-absorption. The latter is an important feature as the level density in the actinides is high and many transitions are of low energy.

It is likewise fortunate that both ^{242}Pu and ^{244}Pu are suitable for use as targets for (d,p) and (d,t) reaction studies. These single-neutron transfer reactions provide a sensitive technique for the identification of specific Nilsson orbitals. This is due to the fact that the transfer cross section is directly dependent on the fine details of the Nilsson wave function, which differs from one orbital to another. Thus in ^{243}Pu one can hope for a rather detailed level scheme encompassing both hole and particle excitations and a large number of of γ-ray transitions.

Section II discusses the experimental procedures and results for the studies of the (n,γ) reaction, including the spin limitations deduced from these data. Section III describes similar information for the studies of the charged-particle reactions, and Sec. IV, using both sets of data, discusses the single-particle Nilsson orbital and rotational band

assignments. Finally, Sec. V discusses these assignments and presents the conclusions from this study.

II. ^{242}Pu$(n,\gamma)^{243}$Pu REACTION

A. Experimental procedures and results

The (n,γ) reaction was studied at the Brookhaven high flux beam reactor. Monoenergetic neutron beams were obtained from a Bragg diffraction crystal monochromator according to a standard experimental arrangement which has been described elsewhere.[10] In the most common mode of operation the neutrons are diffracted from one of the planes of a large Be crystal. The facility provides neutrons in the energy range 0–26 eV with an energy resolution averaging about 15%.

In the principal measurements a sample of ^{242}Pu was bombarded with neutrons whose energy corresponds to that of the lowest resonance at 2.66 eV. The target consisted of 288 mg of plutonium (enriched to 98.26% in ^{242}Pu) embedded in a sulphur matrix, the whole target comprising 2.7189 g of sulphur and plutonium. The target was mounted in a thin walled Al can as a slab approximately 2.5×3.5 cm at 45° to the incident neutron beam. Both high energy (0–6 MeV) and low energy (0–1500 keV) singles γ-ray spectra were recorded with Ge(Li) detectors ranging from 15 to 40 cm^3 in volume. Typical energy resolution was 2.2 keV full width at half maximum (FWHM) for 1.33 MeV γ rays. A 1.5 mm Pb absorber was inserted between target and detector for all runs to reduce pileup resulting from a large number of low energy γ and x rays. The data were stored in a 4096 channel format in a Technical Measurement Corporation multichannel analyzer. All measurements were repeated at least once and the results exhibit excellent reproducibility.

A number of the low energy γ-ray lines and considerable spectral background arose from target radioactivity. In order to accurately subtract these contaminant lines from the γ-ray spectra of interest, test measurements were made of the background target activity prior to any neutron bombardment and subsequently to each run at 2.66 eV. Additionally, an off-resonance measurement at an incident neutron energy of 2.040 eV was made to determine the γ-ray lines from sulphur and from other plutonium isotopes. Some of the contaminant γ-ray lines were helpful in providing a number of accurately known calibration energies below ~1000 keV. These lines were supplemented by those from standard RdTh and ^{60}Co sources as well as by the use of a calibrated pulser. Over most of the energy range 150–1300 keV the cal-

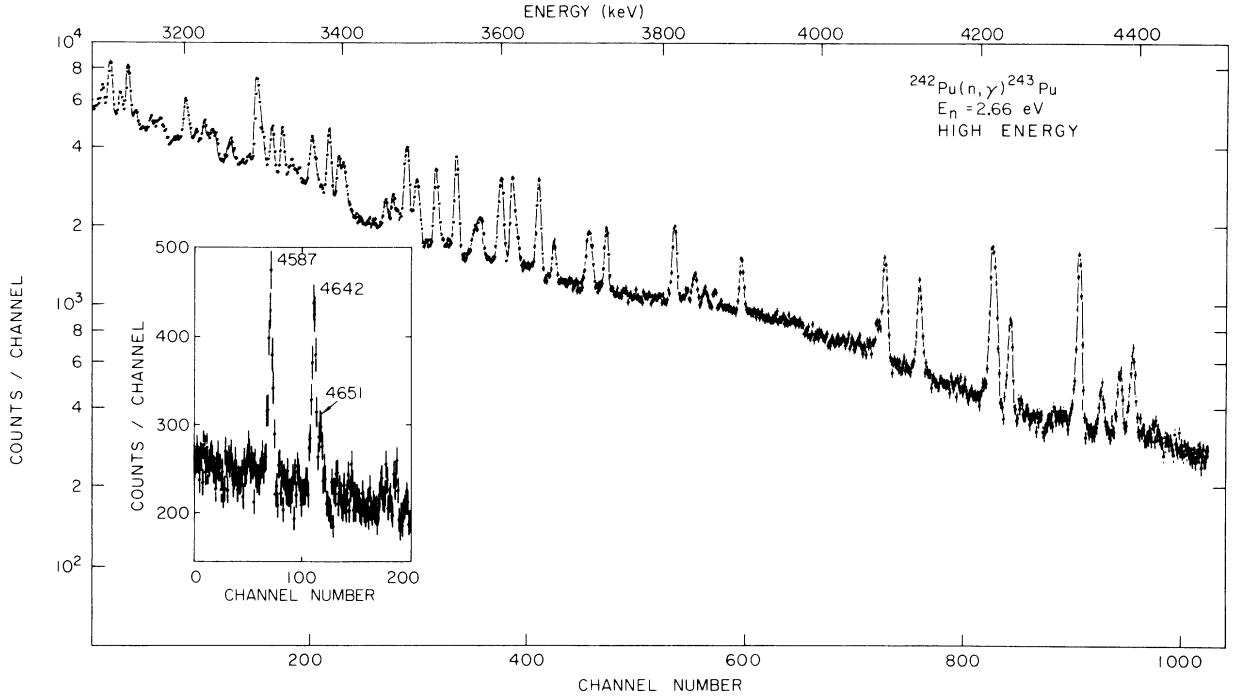

FIG. 1. Portion of a spectrum of high energy γ rays from the ^{242}Pu $(n,\gamma)^{243}$Pu reaction at E_n = 2.66 eV. An energy scale is given along the top axis. The peaks may be either full energy, one or two escape peaks. The insert shows a slightly higher energy region, on a linear scale, that illustrates the splitting of the doublet of primary γ rays populating the 383.6 and 392.3 keV levels. Energy labels are for identification only and are rounded.

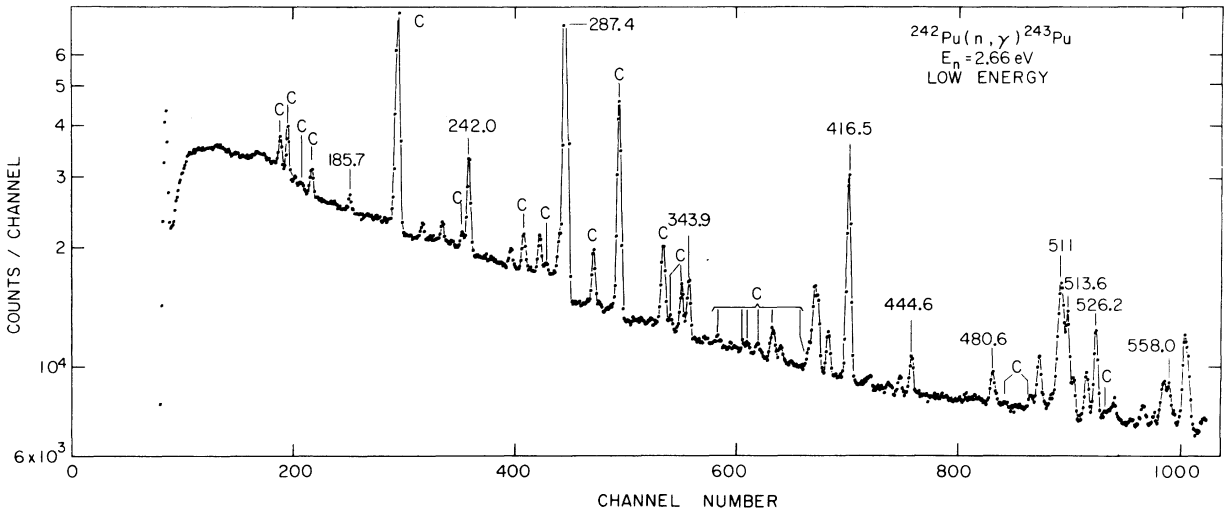

FIG. 2. Portion of a spectrum of low energy γ rays following the ^{242}Pu $(n,\gamma)^{243}$Pu reaction at $E_n = 2.66$ eV. Contaminant γ-ray peaks visible in the spectrum are identified by the letter C. Other, weaker ones, were also identified and contribute some of the spectral background. A few reference γ-ray energies are given.

ibration is accurate to ~±0.2 keV, yielding adopted γ-ray energies with uncertainties usually in the range ±(0.2–0.6) keV, depending on peak size and isolation. For the high energy spectra the calibration in the 3–6 MeV range was established by using the 5.420 MeV γ ray from the ^{32}S(n,γ) reaction, its full energy, first escape, and second escape peaks. An independent and consistent calibration and a finer grained linearity determination were obtained with a precision pulser. Absolute γ-ray energies in this range are accurate to ~±3 keV and the excitation energies extracted from the primary transitions should be reliable to ±1 keV in most cases.

Figures 1 and 2 give examples of portions of the high and low energy γ-ray spectra, respectively. Tables I and II summarize the results of these measurements giving the best values for all γ-ray energies and intensities. The latter are corrected for detector efficiency and for absorption. The absolute intensities were obtained by normalizing to the intensity ($7.0\times10^{-3}/\beta$ decay) of the 381 keV γ ray occurring in the α decay of ^{243}Pu to ^{243}Am. The intensity scale is accurate to ±30%.

In addition to the singles data, γ-γ coincidence data were recorded with both the 15 cm^3 and 40 cm^3 detectors spanning an energy range up to ~1100 keV. The data were stored in event mode format in a 4096×4096 addressable matrix and subsequently analyzed off line with computer programs that construct spectra in either detector in coincidence with events in selected channels from the other detector. Only a few firm coincidence relations could be established and these have been incorporated into the level scheme as indicated by

TABLE I. High energy γ rays from the ^{242}Pu$(n,\gamma)^{243}$Pu reaction at $E_n = 2.66$ eV.

E_γ [a] (keV)	E_{Final} [b] (keV)	I_γ (photons/10^4 capture events) [c]
4650.9	383.3	3.1(6)
4641.9	392.3	8.8
4587.4	446.8	8.3
4381.2	653.0	9.1
4356.9	677.3	6.4
4330.0	704.2	43.5
4243.0	791.2	17.8
4225.0(10)	809.2(10)	20(4)
4220.6	813.6	38.3
4128.6	905.6	24.2
4085.5	948.7	30.3
3903.9	1130.3	16.6
3857.5	1176.7	2.6(9)
3733(1.5)	1301.2(15)	12(3)
3666.4	1367.8	13.0
3646.8	1387.4	42.3
3614(1)	1420.2(10)	39(8)
3599(1)	1435.2(10)	~47 [d]
3543.0	1491.2	50.4
3517.4	1516.8	46.5

[a] Uncertainties are about ±2–3 keV on the absolute energy scale and ±0.8 keV on relative energies unless otherwise specified. The numbers in parentheses are the relative uncertainties, specified where >0.8 keV and are on the last digit.

[b] Deduced excitation energies from the primary transitions, assuming that the 4641.9 keV transition feeds a level at 392.3 keV. This gives a separation energy of $S(n) = 5034.2$ keV. Uncertainties are ±0.8 keV unless otherwise specified in parentheses on the last digit.

[c] Uncertainties are ±15% unless otherwise specified in parentheses on the last digit.

[d] Broad peak.

TABLE II. Low energy γ rays in ^{243}Pu at E_n=2.66 eV.

E_γ (keV) [a]	I_γ (photons/10^3 capture events) [a]	Placement: Initial level	Placement: Final level	Comments [b]
159.2(13)	5 (2)	813.8	654.0	
185.7(7)	14 (4)			
219.9(3)	6 (2)	(873.9	654.0)	
229.3(2)	9 (2)	287.4	58.1	
233.9(6)	2.2(7)	625.6	392.3	
242.0(2)	44 (8)	625.6	383.6	
261.7(3)	6 (2)	654.0	392.3	
275.1(2)	11 (2)	333.2	58.1	
284.4(3)	10 (4)	(677.2	392.3)	
287.4(3)	496 (67)	287.4	0	
333.0(10)	7 (3)	333.2	0	I
343.9(2)	13.2(18)	402.6	58.1 [c]	
		(677.2	333.2)	
		790.7	447.0	
385.7(3)	3.0(5)	1176.5	790.7	
400.8(3)	16.1(18)			
402.6(3)	16.1(18)	402.6	0	
407.1(3)	9.5(11)	790.7	383.6	
416.5(2)	61 (7)	703.9	287.4	
426.0(6)	2.2(7)	809.6	383.6	
		1130.3	703.9	
439.4(3)	2.7(4)	1387.5	948.2	
444.6(3)	7.2(8)			
480.6(3)	5.8(6)	813.8	333.2	
501.2(3)	10.8(12)	948.2	447.0	
513.6(3)	22.8(27)	905.9	392.3	
516.2(3)	6.4(7)			
522.1(3)	7.7(9)	905.9	383.6	
		809.6	287.4	
526.2(3)	18.5(20)	813.8	287.4	
533.9(4)	3.5(7)	981.1	447.0	I
546.9(4)	3.2(16)			
551.7(5)	1.5(4)	(1176.5	625.6)	Q
555.7(5)	9.3(31)	948.2	392.3	I
558.0(3)	8.5(9)	845.4	287.4	
560.3(5)	2.0(7)			
564.7(4)	18.3(20)	948.2	383.6	
566.3(4)	14.3(20)			
573.3(6)	2.1(7)			C(1)
589.1(3)	4.4(5)	981.1	392.3	
600.5(4)	1.6(6)			Q
606.9(6)	1.0(5)			
609.8(3)	5.8(7)			
619.3(7)	0.8(4)			
625.2(2)	5.5(6)	1434.6	809.6	Q
633.8(5)	2.7(4)			C(1)
637.8(3)	2.8(4)			
644.2(4)	2.1(5)	1434.6	790.7	C(1)
648.8(8)	1.9(5)	(981.1	333.2)	C(2)
		(1301.6	654.0)	C(2)

TABLE II *(Continued)*

E_γ (keV) [a]	I_γ (photons/10^3 capture events) [a]	Placement		Comments [b]
		Initial level	Final level	
656.3(2)	5.1(6)			
662.3(5)	6.3(7)			I
663.9(6)	4.5(7)	1367.8	703.9	
668.5(6)	0.9(5)			
676.0(3)	5.1(5)	1301.6	625.6	
679.2(6)	2.5(10)			Q
683.4(4)	3.1(4)	1130.3	447.0	
		1387.5	703.9	
693.5(7)	1.4(5)	981.1	287.4	I
714.7(11)	1.4(7)	(1367.8	654.0)	Q
716.9(5)	1.9(4)	(1420.6	703.9)	
730.1(7)	1.2(4)	1176.5	447.0	
738.2(3)	4.6(5)	1130.3	392.3	
746.4(3)	5.8(6)	1130.3	383.6	
752.7(4)	1.6(5)			
757.5(4)	2.4(4)	1434.6	677.2	
781.1(12)	1.4(9)	(1434.6	654.0)	Q
787.5(8)	2.9(14)	845.4	58.1	
791.3(3)	5.8(15)			
805.9(12)	2.9(9)			C(2)
813.8(2)	17.7(18)	813.8	0	
830.9(5)	1.5(10)			Q, C(2)
838.7(5)	2.1(10)	(1516.5	677.2)	U
841.3(8)	1.7(4)			U
844.3(8)	2.2(4)	(1176.5	333.2)	C(1)
		(845.4	0)	
847.7(3)	5.7(6)			
850.3(3)	5.1(5)			
862.0(8)	4.0(10)			
867.3(3)	5.0(5)			
871.4(5)	2.7(11)			Q
874.1(4)	4.5(5)			
879.8(10)	1.5(7)	(1212.8	333.2)	Q
887.3(6)	9.0(22)			U
889.1(6)	22.3(30)	1176.5	287.4	U
894.6(10)	2.4(8)			C(2)
902.8(4)	8.4(9)			
913.3(3)	6.2(6)			
918.0(10)	2.2(8)	1301.6	383.6	
925.3(10)	2.0(10)	(1212.8	287.4)	U
930.9(12)	3.2(10)			U
976.0(12)	3.8(19)	1367.8	392.3	I, C(2)
999.5(12)	2.0(6)			
1009(1)	2.5(10)			C(3)
1015.6(4)	4.0(5)			
1022.6(4)	5.7(11)			
1028.4(10)	1.2(18)	(1420.6	392.3)	U, Q
1030.9(8)	3.2(13)			U, Q
1042.1(5)	4.0(6)	1434.6	392.3	
1045.0(13)	4.0(18)			

TABLE II *(Continued)*

E_γ (keV) [a]	I_γ (photons/10^3 capture events) [a]	Placement Initial level	Placement Final level	Comments [b]
1050.1(5)	2.3(5)			
1053.8(10)	2.9(11)	1387.5	333.2	U
1055.9(10)	4.1(13)			U
1070.3(4)	2.2(4)			
1087.1(8)	3.1(16)	(1420.6	333.2)	Q
1091.4(6)	5.1(13)			
1162.8(6)	1.9(7)			Q
1169.9(8)	3.1(12)			
1176.5(5)	11.6(24)	1176.5	0	
1180.4(8)	1.3(7)			Q
1191.2(3)	8.3(10)			
1197.6(6)	3.5(14)			
1202.0(3)	5.9(7)			

[a] Errors are on the last digits.

[b] The comments have the following meanings: C(#), denotes a broad peak which is probably a multiplet, the *centroid* energy and *total* intensity being given. The number in parentheses is in keV and gives a guide to the largest possible energy splitting of members of the multiplet; I, line intensity listed may contain a small amount of contaminant intensity remaining after subtraction of a contaminant line on the peak shoulder. For the 333.0 and 555.7 keV lines up to 25% of the listed intensity may be due to contaminant lines. U refers to a pair of lines that are only partially resolved and indicates that the listed values are our best estimates for centroid energies and for intensities of the individual component peaks; Q is a questionable but reproducible line for which a contaminant origin cannot be completely ruled out.

[c] The 402.6-58.1 keV transition was previously observed in the α decay of ^{247}Cm: it is listed with the 343.9 keV line for completeness but comprises only ~0.3 photons/10^3 capture events.

the open dots in the level scheme in Fig. 3.

Delayed coincidence measurements were also carried out. The principal result of these was the detection of a delayed component in the 287.4 keV γ-ray transition. However, no lifetime could be measured for any of the feeding transitions and it is therefore inferred that there is a delayed and highly converted unobserved transition from one or both of the 383.6 and 392.3 keV levels to the state at 287.4 keV. The measured half-life of the delayed component in the 287.4 keV transition was ~300 nsec.

B. Construction of the level scheme

A level scheme, shown in Fig. 3, was constructed from these (n,γ) data which is independent of the charged particle data except as noted specifically below. It is useful to recognize explicitly the rules by which this scheme was established.

For the states below 450 keV, spins and approximate level energies were taken from the existing literature.[11] Precise values for several of these energies were then obtained from strong low energy γ-ray lines. For the levels above 450 keV, deexcitation branches were established from energy combinations and a few coincidence relations. If a level is fed by a primary transition, that is, by a direct transition from the capture state, this provides, initially, a constraint on its excitation energy to within ±1 keV. For levels not populated by primary transitions, approximate energy estimates were obtained from the Q values of (d,t) or (d,p) groups. Once secondary γ-ray transitions were subsequently established, these initial estimates were thereby refined. However, for levels known initially only from the charged particle reactions the likelihood of erroneous accidental energy sums is larger and many transitions involving such states are therefore given as tentative (dctted) in Fig. 3. All lines listed as "questionable" in Table II are classed as tentative in the level scheme. γ rays were generally placed as low as possible in the level scheme since (n,γ) population systematics suggests that low-lying levels are the most strongly populated.

The rules for spin-parity determinations were as follows. As noted, J^π values for known levels

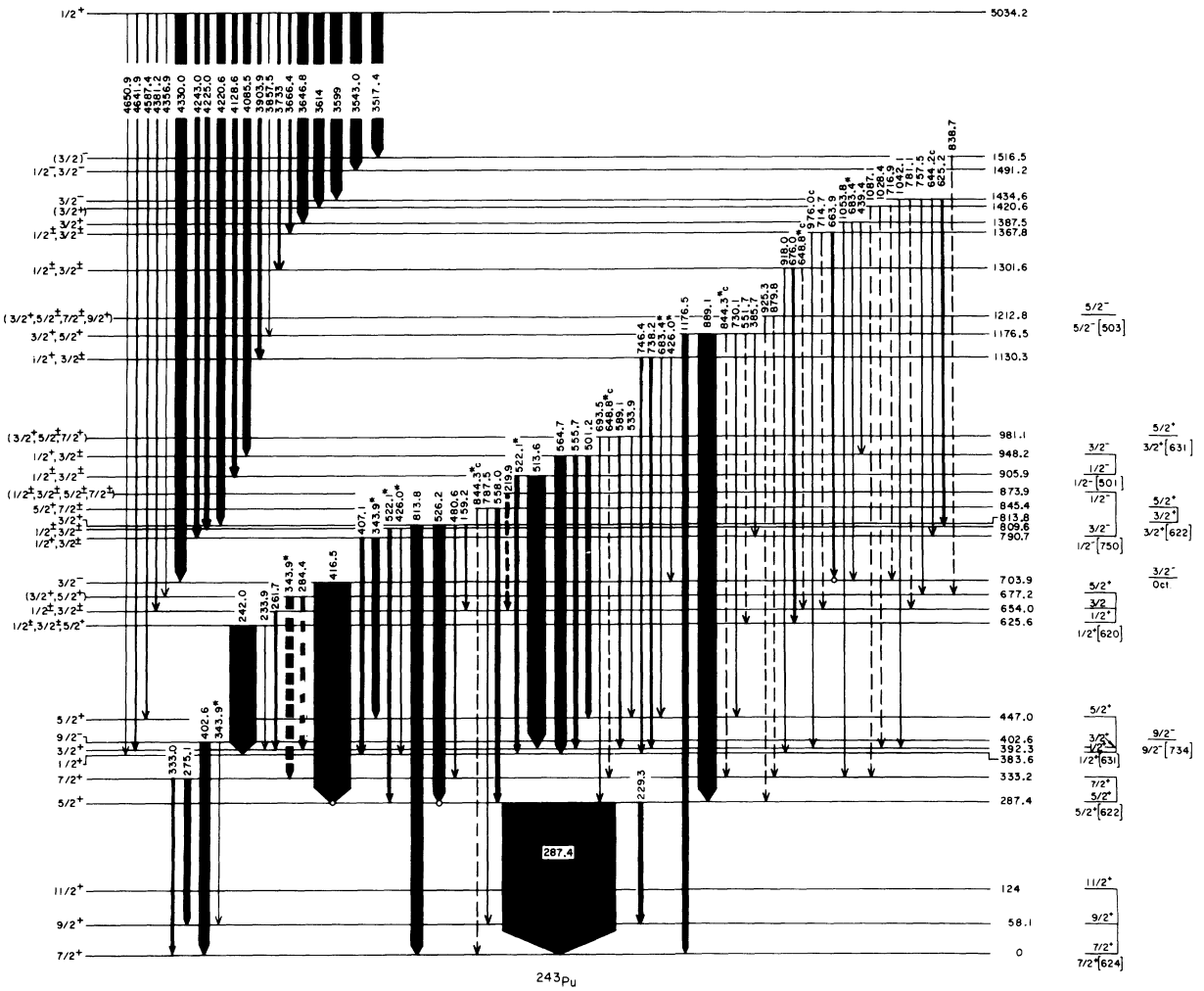

FIG. 3. Level scheme of ^{243}Pu. Above the ground band, the scheme includes only those levels for which information from the (n,γ) reaction was obtained. Others were populated in the (d,p) and (d,t) reactions and are discussed in the text. The widths of the transition arrows are an approximate guide to relative intensity: the scales for primary and secondary γ rays, however, are unrelated. Tables I and II should be consulted for precise intensity values. Open dots terminating certain arrows denote deduced coincidence relations. Dotted transitions are tentative. The labels *c* and * on transitions denote complex peaks and multiply placed transitions respectively. The level spin-parities are deduced only from the (n,γ) data and are discussed in the text. Spin or parity values deduced using dotted transitions are enclosed in parentheses. (See the paragraphs for individual levels for further discussion in these cases.) More precise J^π values are obtained by including the charged particle data. The Nilsson orbital assignments are indicated on the right. See Fig. 6 for a more complete presentation of these band assignments. The current figure provides the best excitation energies for those levels observed in the (n,γ) experiments. For other levels, see Table III.

below 450 keV were taken from existing literature. The capture state spin-parity is $\frac{1}{2}^+$ since the resonance is formed by *s*-wave capture on an even-even target nucleus. The four strongest primary transitions were assumed to be $E1$, and thus the terminal levels are $\frac{1}{2}^-$ or $\frac{3}{2}^-$. Weaker primary transitions could be $M1$ or $E1$ and, for the weakest ($I_\gamma < 7/10^4$ capture events), $E2$ multipolarities were allowed as well. It was assumed that no γ-ray transitions were of $M2$ or higher multipolarity. In support of this assumption we note that $M2$ transitions are spin-allowed in a number of cases but none was observed in the spectra. Thus, for secondary transitions, a γ ray feeding a $\frac{7}{2}^+$ level eliminates $\frac{1}{2}^\pm$ and $\frac{3}{2}^-$ for the initial level. Also, the observation of primary feeding was oc-

casionally used to rule out possible secondary transitions to low lying high spin states that otherwise fit energetically into the level scheme. If tentative (dotted) transitions were used for spin argumentation the resulting J^π value(s) are enclosed in parentheses. See the text for discussion of J^π values obtainable without such transitions. At this stage no account was taken of orbital and band assignments based on (d,p) or (d,t) intensities or "fingerprint patterns" (see Sec. IV), or of the orbital angular momenta implied by the charged particle data with the sole exception of using the $\frac{5}{2}^+$ assignment for the 677.2 keV level to restrict the J^π values for the 1434.6 and 1516.5 keV states. In a subsequent section the J^π assignments of Fig. 3 are refined and band assignments are made on the basis of all existing data.

In the following paragraphs we briefly comment on the individual levels.

Levels below 450 keV

Most of these have been studied before.[11] The low energy γ-ray data obtained here allow the placement of a number of transitions which are consistent with earlier spin assignments and provide some accurate level energies. The (n,γ) data have clarified the nature of the level scheme near 385 keV. The present charged particle data gave evidence of a group near this energy which was ascribed to the $\frac{1}{2}^+[631]$ band. The primary transitions show clearly (see Fig. 1, insert) that a doublet of low spin states exists at ~383 and ~392 keV. Their separation is 9.0 ± 0.5 keV. A 96.2 keV transition to the 287.4 keV level observed in Ref. 12 establishes 383.6 ± 0.3 keV for the energy of one of these two states. For the other state a number of secondary feeding transitions yield an energy of 392.3 ± 0.2 keV. The levels can be assigned as the $\frac{1}{2}^+$ and $\frac{3}{2}^+$ members of the $\frac{1}{2}^+[631]$ rotational band. The close spacing of 9 keV is consistent with the expected decoupling parameter for this orbital. A weak, previously observed, γ-ray branch from the 402.6 keV level to the 124 keV level was below our sensitivity, and that to the 58.1 keV level was obscured by a stronger group.

625.6 keV: $\frac{1}{2}^\pm, \frac{3}{2}^\pm, \frac{5}{2}^+$

No primary transition was observed into this level, whose existence near 625 ± 3 keV is suggested by the charged particle data. It is assumed that it deexcites to the 383.6 keV level by the 242.0 keV transition, a transition which fits nowhere else in the level scheme. Given this, two transitions feeding the 625.6 keV level can be identified, one tentatively.

654.0 keV: $\frac{1}{2}^\pm, \frac{3}{2}^\pm$

The state is fed by a primary transition and deexcites to the 392.3 keV level. The spin limitation is from the primary feeding.

677.2 keV: $(\frac{3}{2}^+, \frac{5}{2}^+)$

The very weak primary feeding implies that the transition can be $E1$, $M1$, or $E2$, thus allowing $J^\pi = \frac{1}{2}^\pm, \frac{3}{2}^\pm, \frac{5}{2}^+$. The tentative transition of 343.9 keV to the $\frac{7}{2}^+$ 333.2 keV level then eliminates $\frac{1}{2}^\pm, \frac{3}{2}^-$ assignments. The only reason for the tentative placement of the 284.4 deexcitation transition is a slight energy imbalance, but within the errors in the γ-ray and level energies involved, the transition does fit.

703.9 keV: $\frac{3}{2}^-$

A very strong primary transition determines negative parity and the 416.5 keV transition to the 287.4 keV $\frac{5}{2}^+$ level, confirmed by a coincidence relation, thereby yields the $\frac{3}{2}^-$ assignment. The level is only populated weakly in the charged particle reactions and does not fit into the expected cross section pattern of any of the plausible single particle orbitals. It may well be of collective octupole character. It is interesting to note that its intense decay to the $J^\pi K = \frac{5}{2}^+\frac{5}{2}$ state at 287.4 keV suggests that $K = \frac{3}{2}$ for the 703.9 keV level.

790.7 keV: $\frac{1}{2}^+, \frac{3}{2}^\pm$

Moderate primary feeding and a transition of 343.9 keV to the $\frac{5}{2}^+$ level at 447.0 keV establishes the spin limitation. Although the 343.9 keV γ ray is close in energy to that of the 402.6 → 58.1 keV transition known[11] from α decay of ^{247}Cm, the contribution of this latter transition to the 343.9 keV group is only ~0.3 photons/10^3 capture events.

809.6 keV: $\frac{1}{2}^\pm, \frac{3}{2}^\pm$; *813.8 keV:* $\frac{3}{2}^+$

A pair of primary transitions of moderate intensity which feed these two closely spaced levels is partially resolved in the primary spectra. Four combinations help define the higher energy level. Two lead to final states of spin-parity $\frac{7}{2}^+$ and thus give the $\frac{3}{2}^+$ assignment. The lower level of the pair is depopulated by two transitions both of which are equally likely placed elsewhere. They are not used in formally limiting further the spin of this state. If the 522.1 keV transition is correctly placed the $\frac{1}{2}^-$ spin possibility for the 809.6 keV level could be eliminated. The particle transfer experiments excite a level (see below) near 810 keV which can be assigned as the $\frac{3}{2}\frac{3}{2}^+[622]$ level. Both the 809.6 and 813.8 keV levels have spin values consistent with the Nilsson assignment.

845.4 keV: $\frac{5}{2}^+, \frac{7}{2}^\pm$

The initial evidence for this level is its observation in the (d, p) and (d, t) reactions. This defines an energy interval of $\pm \sim 3$ keV in which to search for energy combinations. A strong transition, which does not fit elsewhere can be placed as feeding the 287.4 keV level. A tentative ground state transition and one to the 58.1 keV level may also be added. These transitions suggest a spin-parity of $\frac{5}{2}^+$ or higher. A state with $J > \frac{7}{2}$ at this energy is unlikely to be fed with the intensity implied by the γ-ray decay and so we suggest that $J^\pi = \frac{5}{2}^+$ or $\frac{7}{2}^\pm$. It should be noted that this assignment is consistent with the band assignment from the (d, p) and (d, t) reactions (see below).

873.9 keV: $(\frac{1}{2}^\pm, \frac{3}{2}^\pm, \frac{5}{2}^\pm, \frac{7}{2}^\pm)$

A level near this energy is established by the particle data. The only likely deexcitation transition observed has an energy of 219.9 keV. Note that making use of the $\frac{3}{2}\frac{1}{2}^+[620]$ assignment for the 654.0 keV level, one can eliminate the $\frac{7}{2}^-$ spin-parity possibility.

905.9 keV: $\frac{1}{2}^\pm, \frac{3}{2}^\pm$; *948.2 keV:* $\frac{1}{2}^+, \frac{3}{2}^\pm$

These two levels are fed with moderate intensity by primary transitions. Both deexcite strongly by pairs of γ rays to the 383.6 and 392.3 keV levels. The energy difference deduced for the latter two levels from the doublet fitting in the primary γ ray spectrum is supported and confirmed by the splitting of the two pairs of γ rays in the secondary spectrum. A transition of 501.2 keV is also placed as deexciting the 948.2 keV state and it eliminates the $\frac{1}{2}^-$ spin-parity possibility.

981.1 keV: $(\frac{3}{2}^+, \frac{5}{2}^\pm, \frac{7}{2}^+)$

This level is indicated by groups in the particle transfer data. Within a reasonable range for energy combinations, three γ rays can be placed. They define the energy as 981.1 ± 0.3 keV. Using as well a tentatively placed transition feeding the $\frac{7}{2}^+$ level at 333.2 keV level, the J^π values are those shown above. Otherwise $\frac{1}{2}^+$, $\frac{3}{2}^-$ values would also be allowed.

1130.3 keV: $\frac{1}{2}^+, \frac{3}{2}^\pm$

Four deexcitation branches and feeding by a primary γ ray define the spin as above.

1176.5 keV: $\frac{3}{2}^+, \frac{5}{2}^+$

The weak primary population also allows the spin of $\frac{5}{2}^+$. Firmly placed deexcitation transitions to $\frac{5}{2}^+$ and $\frac{7}{2}^+$ levels eliminate J^π values of $\frac{1}{2}^\pm$ and $\frac{3}{2}^-$ leaving $\frac{3}{2}^+$ or $\frac{5}{2}^+$ as possible spin-parities.

Due to the possibility of accumulating uncertainties for levels above 1200 keV, two transitions from any such a level are required before any depopulating transitions from it are classed as firmly placed. Neither of these transitions should fit elsewhere in the level scheme nor should either be itself of "questionable" origin (see Table II).

1212.8 keV: $(\frac{3}{2}^+, \frac{5}{2}^\pm, \frac{7}{2}^\pm, \frac{9}{2}^+)$

Two transitions deexcite this level, whose existence was suggested by the particle transfer data. Unfortunately, one of these lines is questionable and thus our rules require that both transitions be listed as tentative. The spin limits deduced are not very restrictive but are consistent with and support the Nilsson assignment.

1301.6 keV: $\frac{1}{2}^\pm, \frac{3}{2}^\pm$

Three transitions are found to deexcite this level which is populated directly by a moderately strong primary transition.

1367.8 keV: $\frac{1}{2}^\pm, \frac{3}{2}^\pm$

This level is populated by a primary γ ray yielding the above spin-parity limits. The 663.9 keV line is placed with the help of the coincidence data.

1387.5 keV: $\frac{3}{2}^+$; *1420.6 keV:* $(\frac{3}{2}^+)$

Three γ rays are emitted in the decay of each of these levels which are both populated by fairly intense primary transitions. For the 1387.5 keV level one of the secondary transitions feeds the 333.2 keV level, implying a $\frac{3}{2}^+$ assignment for the initial state. Two of the transitions deexciting the 1420.6 keV level are themselves of questionable existence and therefore all three outgoing transitions are left as dotted in Fig. 3. A tentative $(\frac{3}{2}^+)$ assignment relies on the γ-ray transition feeding the $\frac{7}{2}^+$ 333.2 keV level: Otherwise, J^π would be $\frac{1}{2}^\pm$ or $\frac{3}{2}^\pm$.

1434.6 keV: $\frac{3}{2}^-$

One of the most intense primary transitions feeds this level, and five deexcitation branches were observed which limit the spin to $\frac{1}{2}^-$ or $\frac{3}{2}^-$. However, one of these transitions populates the 677.2 keV level. Using the A quality assignment of $\frac{5}{2}, \frac{1}{2}^+[620]$ for the 677.2 keV level excludes the $\frac{1}{2}^-$ spin for the 1434.6 keV state.

1491.2 keV: $\frac{1}{2}^-, \frac{3}{2}^-$

The strongest primary transition establishes the level. No deexciting transitions could be found.

1516.5 keV: $(\frac{3}{2})^-$

This level is also fed strongly be a primary transition and one deexcitation transition could be placed, but it is therefore, by definition, tentative. This transition populates the $\frac{5}{2}, \frac{1}{2}^+[620]$ state at 677.2 keV which argues against the $\frac{1}{2}^-$ spin-parity.

The above spin assignments and restrictions are used below in conjunction with the particle transfer cross sections and angular distributions to suggest Nilsson orbitals and more restrictive spin assignments for many of these states.

III. ^{242}Pu$(d,p)^{243}$Pu AND ^{244}Pu$(d,t)^{243}$Pu REACTIONS

A. Experimental procedure

The experiments were performed with a 12 MeV deuteron beam from the Argonne FN Tandem Van de Graaff accelerator. Proton and triton spectra were analyzed with a split-pole magnetic spectograph.[13] The data were recorded on nuclear emulsions which were later scanned with the Argonne automatic nuclear emulsion scanner.[14] A few peaks were hand scanned to check the automatic scanner. The resulting spectra were analyzed with an automatic spectrum decomposition program. An energy resolution of about 13 keV FWHM was achieved in the (d,p) data and 10 keV FWHM for the (d,t) data. Spectra were measured at 90° and 150° for the (d,p) reaction and at 90°, 120°, and 150° for the (d,t) reaction.

The plutonium targets were prepared by Lerner with the Argonne experimental isotope separator. The separated isotopes were deposited directly onto a self-supporting carbon backing which had been strengthened by adding a thin layer of Formvar. The target material (about 90 μg/cm^2 for ^{242}Pu and about 35 μg/cm^2 for ^{244}Pu) was generally confined to a rectangular area 1×3 mm.

The energy scale of the magnetic spectrograph was calibrated with α particles from a ^{210}Po source, whose energy was taken to be 5.3045 ± 0.005 MeV. The excitation energies for the energy levels seen in the (d,p) spectra were obtained directly from the spectrograph calibration. However, for levels seen in the (d,t) spectra the excitation energies had to be rescaled by about 1 part in 400 to match a few selected energies measured accurately in the (n,γ) part of this study. Presumably, the high magnetic fields used to obtain the (d,t) spectra caused a shift in the energy calibration.

The absolute differential cross sections were measured by comparing the yield observed in the transfer reactions with the yield of deuterons elastically scattered from the target. The deuterons were recorded with a silicon surface-barrier detector mounted at 90° to the beam direction. The ratio of the elastic scattering cross section to that for pure Coulomb scattering was taken to be 0.70 since a measurement[15] of the 90° yields in the scattering of 12 MeV deuterons by ^{238}U had given 0.70 ± 0.03 for this ratio.

B. Experimental results

Spectra measured at 150° with the ^{242}Pu$(d,p)^{243}$Pu and ^{244}Pu$(d,t)^{243}$Pu reactions are shown in Figs. 4 and 5. The several peaks labeled C in Fig. 4 were misidentified in Ref. 2. From their shift in energy with angle, these peaks are known to originate from light mass contaminants in the target. Table III lists the best excitation energies from all the charged data and the differential cross sections measured at 150°. The cross section ratio $d\sigma(90°)/d\sigma(150°)$ is also given. The spin and orbital assignments made in Sec. IV below are also listed for convenience.

The ground-state Q value measured for the ^{244}Pu$(d,t)^{243}$Pu reaction reaction was 0.234 ± 0.005 MeV. The (d,p) Q value is consistent with the absolute γ-ray energies reported in the (n,γ) portion of this paper. Both Q values are consistent with the 1974 Atomic Mass Tables of the Oak Ridge Nuclear Data Project.[16]

IV. ORBITAL AND BAND ASSIGNMENTS

We have used the combined information from the (n,γ) and charged particle reaction data to assign states in ^{243}Pu. This approach is very productive, in particular since not observing a level in one of the two types of experiments can be as informative as observing it in both.

The assignment of the observed levels of the various rotational bands will be discussed in this section as well as our confidence levels[1] for the assignments and the rotational parameters observed for each band. Some of the low-lying particle states in ^{243}Pu have been previously assigned in studies of the α decay of ^{247}Cm[11] and preliminary experiments on the ^{242}Pu$(d,p)^{243}$Pu reaction.[2] We will restate the arguments for their assignments here for the sake of completeness.

The bases of the assignments are given in detail in Ref. 1 but will be briefly reviewed here. They are as follows:

(1) The "signature" or "fingerprint pattern" of the state, i.e., the cross sections and energy spacings of the various rotational levels in each band. Since the cross sections are directly related to the wave functions, they can provide unique assignments for each band. A catalog of

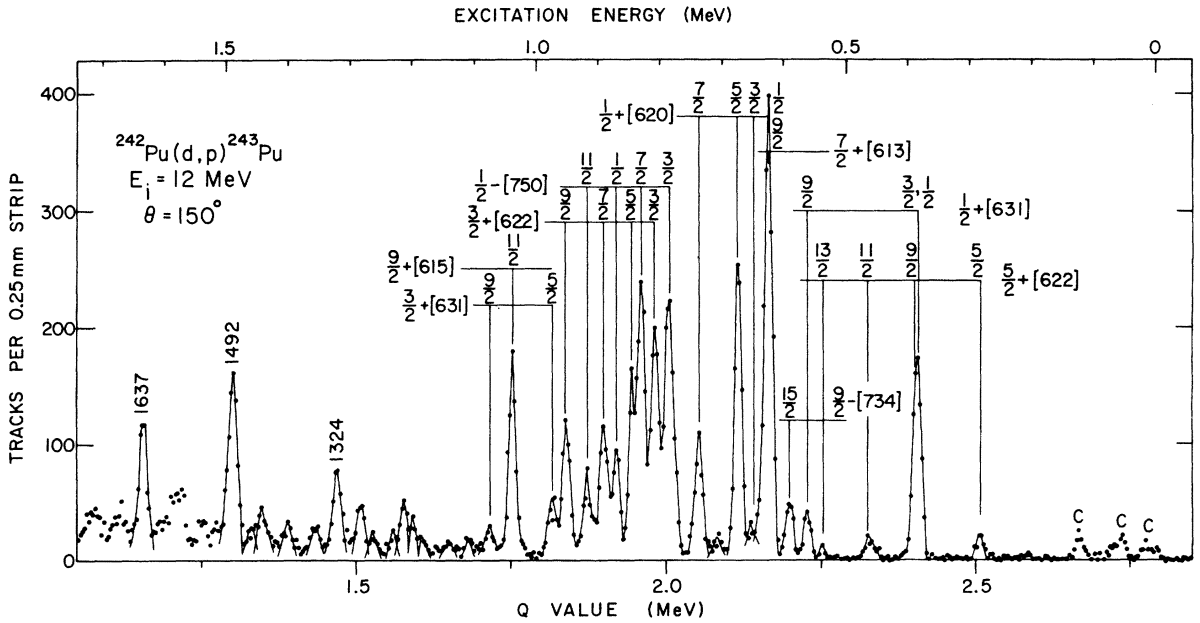

FIG. 4. Proton spectrum from the ^{242}Pu$(d,p)^{243}$Pu reaction. Orbital and spin assignments are shown. Contaminant peaks are labeled C.

theoretical and experimental "signatures" is given in Fig. 4 of Ref. 1.

(2) The ratio of (d, p) to (d, t) cross sections R of the ^{242}Pu$(d, p)^{243}$Pu and ^{244}Pu$(d, t)^{243}$Pu transitions populating each state. This ratio will often identify particle ($R \gg 1$) and hole ($R \ll 1$) states as well as collective states.

(3) The ratio of the differential cross sections at two angles 90° and 150° frequently supplies an important clue as to the l value of the transition. Generally, a small value of the ratio $d\sigma(90°)/d\sigma(150°)$ implies a large value of l.

(4) The spin limitations implied by the transitions seen in the (n,γ) experiments and discussed

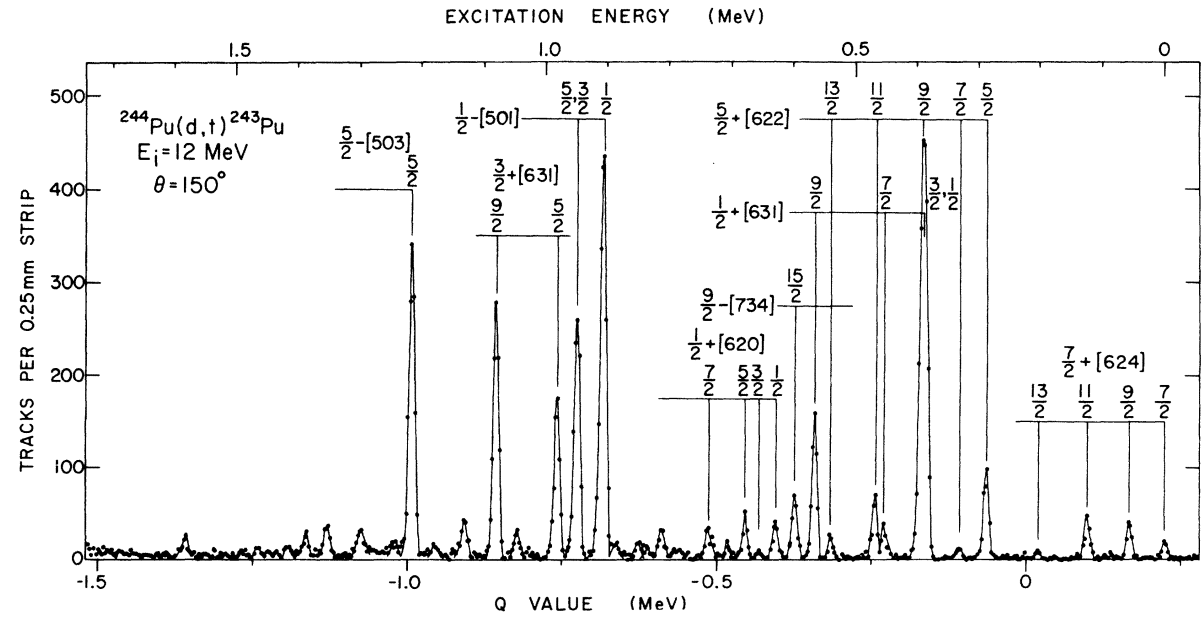

FIG. 5. Triton spectrum from the ^{244}Pu$(d,t)^{243}$Pu reaction. Orbital and spin assignments are shown.

TABLE III. Energy levels in ^{243}Pu, their excitation energies, differential cross sections in (d,p) and (d,t) reactions, cross-section ratios at 90° and 150°, and orbital assignments.

Excitation energy (keV)	(d,p) $d\sigma/d\Omega$ [a] at 150° (μb/sr)	(d,p) $\frac{d\sigma(90°)}{d\sigma(150°)}$	(d,t) $d\sigma/d\Omega$ [a] at 150° (μb/sr)	(d,t) $\frac{d\sigma(90°)}{d\sigma(150°)}$	Assignment J	Assignment Orbital	Confidence
0	<2		11.4	0.56	$\frac{7}{2}$	$\frac{7}{2}^+$[624]	A
55.6 ± 1.5	<2		27.3	0.54	$\frac{9}{2}$	$\frac{7}{2}^+$[624]	A
123.7 ± 1.5	<2		29.5	0.34	$\frac{11}{2}$	$\frac{7}{2}^+$[624]	A
204.4 ± 1.5	<2		4.8	~0.20	$\frac{13}{2}$	$\frac{7}{2}^+$[624]	A
287.7 ± 1.5	10.0	1.7	68.5	0.90	$\frac{5}{2}$	$\frac{5}{2}^+$[622]	A
330.9 ± 1.5	<1		8.1	0.55	$\frac{7}{2}$	$\frac{5}{2}^+$[622]	A
388 ± 3 [b]	92 [b]	1.3	456 [b]	0.80	$\frac{1}{2}, \frac{3}{2}$	$\frac{1}{2}^+$[631]	A
					$\frac{9}{2}$	$\frac{5}{2}^+$[622]	A
450.1 ± 1.5	<2		22	0.46	$\frac{7}{2}$	$\frac{1}{2}^+$[631]	A
466.7 ± 1.5	10.0	1.3	42.7	0.52	$\frac{11}{2}$	$\frac{5}{2}^+$[622]	A
536.6 ± 1.5	3.8	<0.6	15.5	~0.15	$\frac{13}{2}$	$\frac{5}{2}^+$[622]	A
564.5 ± 1.5	19.3	0.9	108	0.43	$\frac{9}{2}$	$\frac{1}{2}^+$[631]	A
595.3 ± 1.5	25.5	0.33	47.2	0.15	$\frac{15}{2}$	$\frac{9}{2}^-$[734]	C
625.6 [c]					$\frac{1}{2}$	$\frac{1}{2}^+$[620]	A
626 ± 2 [d]	194 [d]	1.3	29.8 [d]	0.90	$\frac{9}{2}$	$\frac{7}{2}^+$[613]	B
651 ± 2	15	~1.5	4.3	~0.6	$\frac{3}{2}$	$\frac{1}{2}^+$[620]	A
676.3 ± 1.5	115	1.3	28.9	0.50	$\frac{5}{2}$	$\frac{1}{2}^+$[620]	A
704.5 ± 1.5	10.6	0.68	9.3	0.78		Octupole	
734.1 ± 2	<15		10	0.25			
741.8 ± 1.5	52.5	0.91	15	0.25	$\frac{7}{2}$	$\frac{1}{2}^+$[620]	A
790.4 ± 1.5	127	1.55	7.4	1.1	$\frac{3}{2}$	$\frac{1}{2}^-$[750]	B
811.6 ± 1.5	102	1.55	22.8	0.63	$\frac{3}{2}$	$\frac{3}{2}^+$[622]	B
834.4 ± 1.5	108	1.58	7.8	1.02	$\frac{7}{2}$	$\frac{1}{2}^-$[750]	B
849.2 ± 1.5	66.7	0.8	10	0.89	$\frac{5}{2}$	$\frac{3}{2}^+$[622]	B
874.2 ± 1.5	45.3	1.43	<3		$\frac{1}{2}$	$\frac{1}{2}^-$[750]	B
884 ± 3	<30		9.7	0.8			
895.6 ± 1.5	58.4	0.98	<12		$\frac{7}{2}$	$\frac{3}{2}^+$[622]	B
905.1 ± 1.5	<30		360	0.55	$\frac{1}{2}$	$\frac{1}{2}^-$[501]	A
920.6 ± 1.5	35.7	0.88	<6		$\frac{11}{2}$	$\frac{1}{2}^-$[750]	B
948.8 ± 1.5	<15		204	0.52	$\frac{3}{2}, \frac{5}{2}$	$\frac{1}{2}^-$[501]	A
954 ± 2	60.8	0.86	<12		$\frac{9}{2}$	$\frac{3}{2}^+$[622]	B
982 ± 2	24.5	1.47	124	0.59	$\frac{5}{2}$	$\frac{3}{2}^+$[631]	B
1044 ± 2	81.4	0.70	20.4	~0.17	$\frac{11}{2}$	$\frac{9}{2}^+$[615]	C
1080 ± 2	14.1	1.0	204	0.37	$\frac{9}{2}$	$\frac{3}{2}^+$[631]	B
1114 ± 3	9.4	~0.5	<3				
1131 ± 2	<4		32.2	0.53			
1145 ± 3	7	~0.3	<6				

TABLE III (*Continued*)

Excitation energy (keV)	(*d*,*p*) $d\sigma/d\Omega$ [a] at 150° (μb/sr)	(*d*,*p*) $\frac{d\sigma(90°)}{d\sigma(150°)}$	(*d*,*t*) $d\sigma/d\Omega$ [a] at 150° (μb/sr)	(*d*,*t*) $\frac{d\sigma(90°)}{d\sigma(150°)}$	Assignment *J*	Assignment Orbital	Confidence
1178 ±2	6	~0.3	9.1	0.63			
1197 ±3	13	1.8	<4				
1216 ±3	22	1.4	268	0.53	$\frac{5}{2}$	$\frac{5}{2}^-$[503]	C
1233 ±3	8.6	1.7	<6				
1243 ±3	<4		13.5	0.45			
1265 ±3	8.8	1.3	<6				
1286 ±3	24.3	1.1	<6				
1299 ±2	<6		24.5	~0.2			
1324 ±2	39.6	0.88	<6				
1354 ±2	<7		27.0	~0.22			
1359 ±3	14.3	~1.0	<9				
1389 ±2	<4		17.4	0.44			
1403 ±3	13.7	1.6	<4				
1419 ±3	<6		8.2	0.46			
1444 ±3	22	0.8	4.9	~0.5			
1465 ±3	8	~1.0	6.3	~0.5			
1492 ±2	85	1.3	<3				

[a] The uncertainty in the cross section of the strongly excited levels is about 15%.
[b] Unresolved triplet.
[c] Energy from (n,γ) measurement.
[d] Unresolved doublet.

in Sec. II for each observed level. In addition, these transitions sometimes imply limitations on the angular momentum projection quantum number K: such limitations, being model dependent and nonrigorous, are cited below only in the sense of providing supporting evidence.

(5) We will also use information obtained in decay studies and reaction spectroscopic studies of nearby nuclei to suggest energy orderings and approximate level spacings.

The various rotational bands will be discussed in order of increasing excitation energy. The band assignments are illustrated in Fig. 6.

$\frac{7}{2}^+[624]$

The $J=\frac{7}{2}$, $\frac{9}{2}$, and $\frac{11}{2}$ levels of this band were seen in the α decay[11] of ^{247}Cm. The excitation energies of these levels measured with the (d,t) reaction, 55.6 and 123.7 keV, agree well with these assignments. Also the relative cross sections for these transitions are the same as the calculated "signature" for this state and with the "signature" for it as observed[2,1] in ^{241}Pu and ^{235}U. The observed rotational constant of 6.2 keV leads to the prediction of an excitation energy of 205.2 keV for the $J=\frac{13}{2}$ state of this band, and the transition to the level at 204.4±1.5 keV has the appropriate cross section and energy for this state. For these reasons these levels are assigned with an A confidence level.

$\frac{5}{2}^+[622]$

The $J=\frac{5}{2}$ and $\frac{7}{2}$ levels of this band were observed and identified in the α-decay studies of Ref. 11. If a rotational constant of 6.2 keV is assumed, this would imply that the $J=\frac{9}{2}$, $\frac{11}{2}$, and $\frac{13}{2}$ levels of this band would be at 387, 456, and 536 keV. Both the (d,p) and (d,t) spectra show a particle group with a centroid at 388±3 keV excitation whose width is greater than those of the adjacent peaks. Part of this complex group is presumably the $\frac{9}{2}\,\frac{5}{2}^+[622]$ level. Other members of the $\frac{5}{2}^+[622]$ band are presumably levels observed at 466.7 and 536.6 keV, which lie close to the predicted energies and have cross sections of the size predicted.

$\frac{1}{2}^+[631]$

The 0.33 μsec isomeric transition from the $J^\pi=\frac{1}{2}^+$ level of this band has been observed by Yates *et al.*[12] They assigned this transition to a level with an excitation energy of 384 keV which is presumably seen as part of the complex group observed at 388 keV in the transfer data and at 383.6 keV in the (n,γ) experiment. The latter measurements show the existence in fact of two

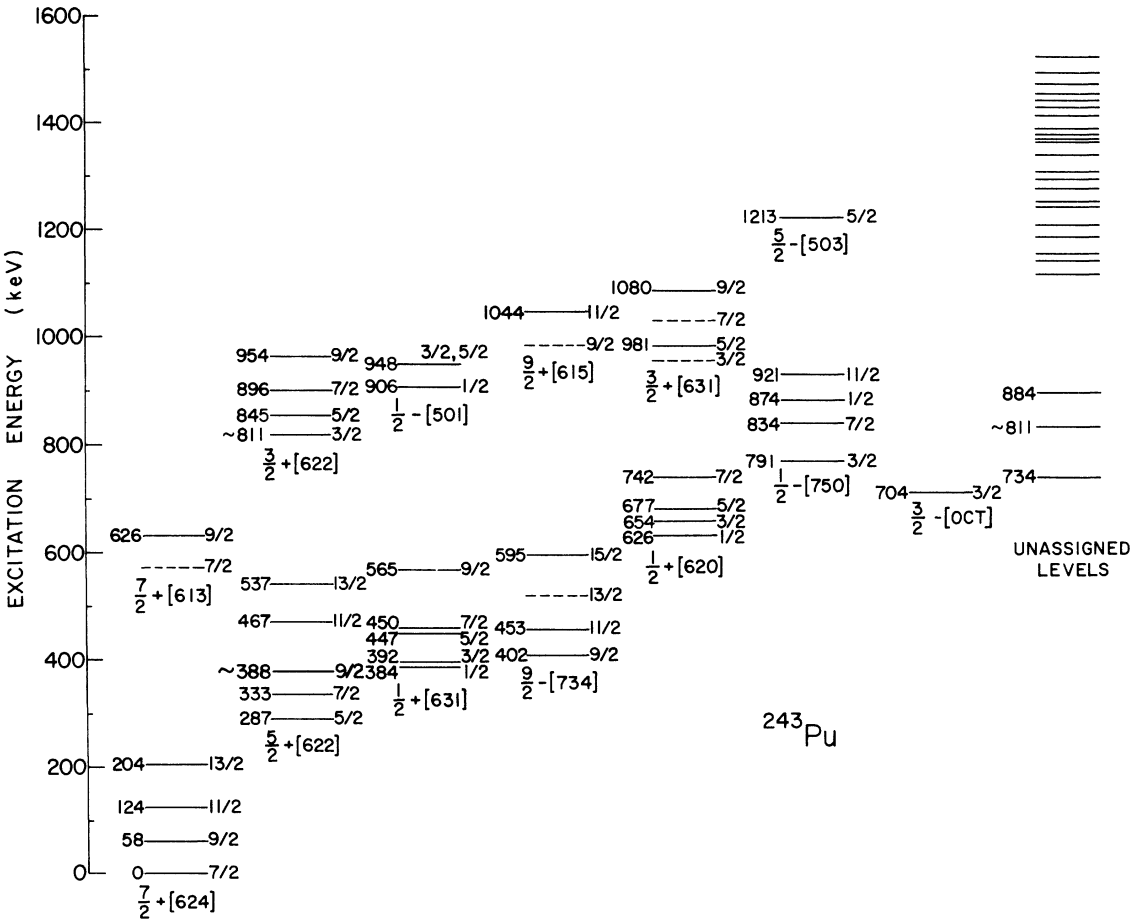

FIG. 6. Energy level diagram of ^{243}Pu showing rotational-band structure, orbital and spin assignments.

levels, at 383.6 and 392.3 keV, which we assign as the $\frac{1}{2}^+$ and $\frac{3}{2}^+$ band members. The cross sections of the remaining levels of this band fit the expected "signature" of the $\frac{1}{2}^+[631]$ state. For these reasons, this band is assigned an A confidence level.

$\frac{9}{2}^-[734]$

The only particle transition observed to a level in this band is the (d,t) population of the $J^\pi = \frac{15}{2}^-$ level at 595.3 keV. The rotational constant 5.55 keV, calculated from the energies of the $J = \frac{9}{2}$ and $\frac{11}{2}$ levels seen in α decay, leads to a prediction of an excitation energy of 618 keV for the $J = \frac{15}{2}$ level. However, Coriolis mixing with the $\frac{7}{2}^-[734]$ and $\frac{11}{2}^-[725]$ bands (which, though unobserved, are expected to be at 1–2 MeV of excitation) could easily lower the excitation energy of the $J = \frac{15}{2}$ level. The angular distribution of the (d,t) transition populating this level indicates that it has a high spin. We are assigning the $J = \frac{15}{2}$ level a confidence value of B.

$\frac{1}{2}^+[620]$

The population of levels in the (n,γ) reaction at 625.6, 654.0, and 677.2 keV, with their deduced spin limitations, and the correspondence of the "signature" of the (d,p) transitions to the $J = \frac{1}{2}$, $\frac{3}{2}$, $\frac{5}{2}$, and $\frac{7}{2}$ levels of this band to that predicted and also observed elsewhere in the actinides, makes the assignment of this excitation unambiguous (A confidence level).

$\frac{7}{2}^+[613]$

Only the $J = \frac{9}{2}$ level of this band is populated in the (d,p) and (d,t) reactions, and it is degenerate with the $\frac{1}{2}\frac{1}{2}^+[620]$ level. But this is the expected "signature" and cross section based on evidence from other actinide elements.[1,3] There is no ob-

served population in the (n,γ) experiment as would be expected. The ratio of the $(d,p)/(d,t)$ cross section of the unresolved group at 626 keV excitation energy, which presumably contains both the $\frac{9}{2}\frac{7}{2}^+[613]$ and $\frac{1}{2}\frac{1}{2}^+[620]$ levels, strongly suggests that both levels belong to particle excitations.

$\frac{1}{2}^-[750]$

The "signature" of this band for the $J=\frac{3}{2}$, $\frac{7}{2}$, and $\frac{11}{2}$ levels was observed[3] in ^{245}Cm, ^{247}Cm, and ^{249}Cm and was essentially the same as seen here, except that, in addition, the $J=\frac{1}{2}$ level is observed in ^{243}Pu presumably because a cleaner spectrum was obtained. Both the $J=\frac{3}{2}$ and $\frac{1}{2}$ levels seem to be observed in the (n,γ) reaction at 790.7 and 873.9 keV. A fit to the energies gives a decoupling constant of -4.1 and a rotational constant of 8.1 keV, which is somewhat larger than expected. While it should be noted that, unlike the case[2] of ^{241}Pu, there is not a high degree of fragmentation, there still may be enough residual interaction to yield these anomalous rotational parameters. This band is assigned a confidence level of B.

$\frac{3}{2}^+[622]$

The cross sections for the (d,p) transitions to the levels of this band fit those predicted for the signature. In addition, the capture γ-ray cascades yield $J^\pi=\frac{1}{2}$ or $\frac{3}{2}$ and $\frac{5}{2}^+$ or $\frac{7}{2}^-$ for the first two rotational levels and the ratio R is correct for a particle excitation at this energy. Also, the transition from the 845.4 keV to the 58.1 keV level supports a K value $\geq\frac{3}{2}$. For these reasons, we are assigning this band a confidence level of B.

$\frac{1}{2}^-[501]$

The large (d,t) cross section, and spin assignments resulting from the capture γ-ray cascade, all fit the assignment of this band. Since it agrees so well with the "signature" observed in most of the actinide region, it is given an A confidence level. It should be noted that, unlike the case in ^{241}Pu, there is no large amount of mixing with the $\frac{1}{2}^-[750]$ band.

$\frac{3}{2}^+[631]$

The "signature" of this hole state extracted from the (d,t) data resembles that seen elsewhere[1,3] for the $J=\frac{5}{2}$ and $\frac{9}{2}$ levels of this band. In addition, the (n,γ) data are consistent with a spin of $\frac{5}{2}$ and suggest $K=\frac{3}{2}$ or $\frac{5}{2}$ for the 981.1 keV state which we assign as the $\frac{5}{2}^+$ level of the band. However, there is no (observed) population of the $J=\frac{3}{2}$ level in the (n,γ) experiment. We are assigning the band a B confidence level.

$\frac{9}{2}^+[615]$

The predicted "signature" of this band, which requires a low cross-section transition to the $J=\frac{9}{2}$ level and a high cross-section transition to the $J=\frac{11}{2}$ level, is too indeterminate for specific assignment. In fact, it is only the angular dependence of the $l=6$ transition to the $J=\frac{11}{2}$ state that aids in identification. The 1044 keV level fits this assignment but the criteria are so vague that only a confidence level of C is given.

$\frac{5}{2}^-[503]$

The level at 1216 ± 3 keV appears to be a hole state and is populated by a single, strong, low l transition in the (d,t) experiments. The only hole states in this energy region that have predicted cross sections to fit this signature are the $\frac{5}{2}^-[503]$ and $\frac{3}{2}^-[501]$. Of these the J^π restrictions from the (n,γ) data only allow the former assignment. However, this state is given a confidence level of C because of the incompleteness of information.

V. DISCUSSION

A. Comparison of relative γ-ray transition probabilities with the Nilsson model

It is of interest to use the band assignments of the previous section to reconsider the deexcitation γ-ray branches deduced in Sec. II. We shall deal first with a qualitative analysis, turning subsequently to some quantitative predictions.

The simplest analysis is to check for violations and implications of the K selection rules. The Nilsson assignments provide K quantum numbers for a large number of levels, and the spin-parity limitations deduced in the (n,γ) experiments for other levels provide limitations on possible K values. In considering the assigned transitions in light of the K selection rules, we assume that they proceed by either $E1$, mixed $M1$, $E2$, or $E2$ radiation, as allowed by the J^π values involved.

One concludes that none of the 63 lines placed in the level scheme is definitely K forbidden for any of the J^π values allowed by Fig. 3. However, further analysis allow some additional restrictions on K values. In two cases, as noted in Sec. IV, these provide supporting evidence for the Nilsson assignments made and in no case is there a conflict with those assignments. Other cases where limitations on K values are possible are as follows.

1. The 703.9 keV level decays intensely to the 287.4, $K=\frac{5}{2}$ state by a presumably $E1$ transition.

This suggests that the K value of the 703.9 keV level is $\frac{3}{2}$ and supports the interpretation that it is an octupole vibration, built either on the $\frac{7}{2}^+[624]$ or $\frac{5}{2}^+[622]$ orbital. In the neighboring even-even nuclei both experiment and microscopic calculations[17] in fact suggest that the lowest octupole vibrations have $K=1$ or 2 and occur between 500 and 1000 keV of excitation energy. It might be noted that a $K=\frac{5}{2}$ octupole vibration is ^{243}Pu would probably not be evident in these experiments since the charged particle cross section is likely to be small and there would be no primary population. The definition of acceptable levels for which γ-ray combinations were sought required one or both of these conditions: *new* levels were *not* proposed solely on the basis of consistent energy combinations.

2. If the 809.6 keV level has odd parity, the 522.1 keV transition suggests that $K=\frac{3}{2}$, but if it is identical with the nearby even parity state populated in the charged particle reactions, K can be either $\frac{1}{2}$ or $\frac{3}{2}$, the latter being that of the $\frac{3}{2}^+[622]$ Nilsson orbital assigned to either this or the 813.8 keV state.

3. The ground state transition from the 813.8 keV state implies that $K=\frac{3}{2}$.

4. The ground state transition from the 1176.5 keV state determines that $K\geq\frac{3}{2}$, while the large matrix element inferred from the low energy transition to the $\frac{1}{2}^-[750]$ band member at 790.7 keV implies that $K=\frac{1}{2},\frac{3}{2}$; $K=\frac{3}{2}$ is thus the consistent choice. If the state is $\frac{3}{2}^+$, it is then a bandhead and we note in fact that a $J^\pi=\frac{3}{2}^+$ rather than $\frac{5}{2}^+$ choice is suggested by comparison of the transition rates from this level with the Alaga rules[18] (See Table IV.).

There are five odd parity states for which the Nilsson assignments allow a more detailed treatment. These are at 402.6 keV ($\frac{9}{2}\frac{9}{2}^-[734]$), 790.7 keV ($\frac{3}{2}\frac{1}{2}^-[750]$), 905.9 and 948.2 keV ($\frac{1}{2}$ and $\frac{3}{2}\frac{1}{2}^-[501]$, respectively), and 1212.8 keV ($\frac{5}{2}\frac{5}{2}^-[503]$). From the first, Fig. 3 shows that the only detectable γ radiation (that is, above our low energy cutoff of 150 keV) would consist of transitions to the ground band. Table IV compares the decay of some levels with the relative transition probabilities calculated from the Alaga ratios. As is evident, the agreement is rather good for the 402.6 keV state.

The depopulation of the 1212.8 keV level only to a $K=\frac{5}{2}$ band is consistent with the $\frac{5}{2}\frac{5}{2}^-[503]$ assignment given above. In fact, with this assignment, the branching ratio for this state is in good agreement with the Alaga rules as shown in Table IV; it is in disagreement for a $K=\frac{3}{2}$ choice. The preference for the deexcitation of the 1212.8 keV level to the $\frac{5}{2}^+[622]$ band is reasonable. Branches to the two lower lying even parity $K=\frac{1}{2}$ bands would be forbidden, those to the $\frac{3}{2}^+[622]$ band would be $E1$ and therefore strongly retarded by the pairing correlations[19] for electric transitions between levels on opposite sides of the Fermi surface $[P\sim(u_1u_2-v_1v_2)^2]$. Branches to the $\frac{7}{2}^+[624]$ band would also be slowed by pairing effects but could also have been comparable in intensity to the two lines placed and have escaped tabulation since only the strong and unambiguous lines were analyzed above 1100 keV. Low energy branches to the $\frac{1}{2}^-[501]$ band and to the $\frac{5}{2}\frac{3}{2}^+[631]$ level at 981.1 keV would be highly retarded relative to those feeding the $\frac{5}{2}^+[622]$ band by the $E_\gamma{}^3$ factor, and the latter would be further retarded by the $\Delta n_z=3$ and $\Delta\Lambda=2$ changes that would be required in the asymptotic Nilsson quantum numbers.

No Alaga rule comparisons can be made for the other odd parity levels because they decay by presumably $E1$ radiation between initial and final levels with $K=\frac{1}{2}$. For such a case of $L=K_i+K_f$ the transition probability expressions contain an additional term and the simple Alaga rules are not obtainable by cancellation. However, as above, the asymptotic selection rules for decay based on the Nilsson assignments provide clues to their likely expected decay routes.

Empirically, the 790.7 keV level deexcites by K allowed transitions only to the $\frac{1}{2}^+[631]$ band (cf. Fig. 3). The alternative terminal levels are those belonging to the $\frac{7}{2}^+[624]$, $\frac{5}{2}^+[622]$, $\frac{9}{2}^-[734]$, and $\frac{1}{2}^+[620]$ bands. Decay to the first and third requires multipolarities at least as high as $M2,E3$ and $M3,E4$, respectively, and would not be expected to compete with possible $E1$ routes. Weak low energy decay branches to the $\frac{1}{2}^+[620]$ band might well have been missed in the γ-ray spectra, but in any case should be weak because of the low energy and the $\Delta n_z=3$ hindrance. Finally, decay radiation to the $\frac{5}{2}\frac{5}{2}^+[622]$ level would be once K forbidden if $E1$ or else must be $M2$. In addition there would be a $\Delta n_z=3$ and $\Delta\Lambda=2$ change in asymptotic quantum numbers.

The 905.9 and 948.2 keV levels of the $\frac{1}{2}^-[501]$ band deexcite intensely to the $\frac{1}{2}^+[631]$ band. This involves a $\Delta n_z=3$ hindrance. The former level can decay to the $\frac{5}{2}^+[622]$ and $\frac{7}{2}^+[624]$ bands only by $M2$, $E3$, and $E3$ radiation, respectively. This is also true for the 948.2 keV level except that an $E1$ transition which would be once K forbidden could feed the $\frac{5}{2}\frac{5}{2}^+[622]$ level. However, we have carried out Coriolis mixing calculations that show that the latter (287.4 keV) state does not mix appreciably with either of the $K^\pi=\frac{3}{2}^+$ orbitals near 900 keV. This is confirmed by the particle transfer cross sections to the 905.9 and 948.2 keV levels which suggest little mixing and fragmentation of the $\frac{1}{2}^-[501]$ orbital itself. The only other plausible decay routes for these two states are to the $\frac{1}{2}^+[620]$ band near 650 keV. However, these $E1$ transitions

TABLE IV. Comparison of measured relative γ-ray transition rates with the symmetric rotor model.

Initial level		Final level		Relative γ-ray transition rate [b] Rotor model		
E (keV)	$JK^{\pi}[Nn_z\Lambda]$ [a]	E (keV)	$JK^{\pi}[Nn_z\Lambda]$ [a]	Dipole	Quadrupole	Exp.
287.4	$\frac{5}{2}\frac{5}{2}^+[622]$	0	$\frac{7}{2}\frac{7}{2}^+[624]$	1.0	1.0	1.0
		58.1	$\frac{9}{2}\frac{7}{2}^+[624]$	0	0.26	0.018
333.2	$\frac{7}{2}\frac{5}{2}^+[622]$	0	$\frac{7}{2}\frac{7}{2}^+[624]$	0.51	11.4	0.67
		58.1	$\frac{9}{2}\frac{7}{2}^+[624]$	1.0	1.0	1.0
		124	$\frac{11}{2}\frac{7}{2}^+[624]$	0	1.41	c
402.6	$\frac{9}{2}\frac{9}{2}^-[734]$	0	$\frac{7}{2}\frac{7}{2}^+[624]$	1.0	1.0	1.0
		58.1	$\frac{9}{2}\frac{7}{2}^+[624]$	0.14	0.33	0.02
		124	$\frac{11}{2}\frac{7}{2}^+[624]$	0.007	0.035	<0.19
703.9	$\frac{3}{2}\frac{3}{2}^-$	287.4	$\frac{5}{2}\frac{5}{2}^+[622]$	1.0	1.0	1.0
		333.2	$\frac{7}{2}\frac{5}{2}^+[622]$	0	0.75	<0.02
813.8	$\frac{3}{2}\frac{3}{2}^+[622]$	287.4	$\frac{5}{2}\frac{5}{2}^+[622]$	1.0	1.0	1.0
		333.2	$\frac{7}{2}\frac{5}{2}^+[622]$	0	0.85	0.32
981.1	$\frac{5}{2}\frac{3}{2}^+[631]$	383.6	$\frac{1}{2}\frac{1}{2}^+[631]$	0	d	<0.61
		392.3	$\frac{3}{2}\frac{1}{2}^+[631]$	1.0		1.0
		447.0	$\frac{5}{2}\frac{1}{2}^+[631]$	0.85		0.80
1176.5	$\frac{3}{2}\frac{3}{2}^+$	287.4	$\frac{5}{2}\frac{5}{2}^+[622]$	1.0	1.0	1.0
		333.2	$\frac{7}{2}\frac{5}{2}^+[622]$	0	1.02	0.10*
		388	$\frac{9}{2}\frac{5}{2}^+[622]$	0	0	<0.08
		0	$\frac{7}{2}\frac{7}{2}^+[624]$	0	1.0	1.0
		58.1	$\frac{9}{2}\frac{7}{2}^+[624]$	0	0	<0.20
	$\frac{5}{2}\frac{3}{2}^+$	287.4	$\frac{5}{2}\frac{5}{2}^+[622]$	0.47	1.0	1.0
		333.2	$\frac{7}{2}\frac{5}{2}^+[622]$	1.0	0.028	0.10*
		388	$\frac{9}{2}\frac{5}{2}^+[622]$	0	0.69	<0.08
		0	$\frac{7}{2}\frac{7}{2}^+[624]$	0	1.0	1.0
		58.1	$\frac{9}{2}\frac{7}{2}^+[624]$	0	0.97	<0.20
1212.8	$\frac{5}{2}\frac{5}{2}^-[503]$	287.4	$\frac{5}{2}\frac{5}{2}^+[622]$	1.0	1.0	1.0
		333.2	$\frac{7}{2}\frac{5}{2}^+[622]$	0.34	1.04	0.77
		388	$\frac{9}{2}\frac{5}{2}^+[622]$	0	0.26	<0.60

[a] The $J^{\pi}K$ values used in the table are for test purposes and are *not* necessarily the assigned values. The latter are contained in Figs. 3 and 6 and in Table III. Similarly, the Nilsson assignments are listed (where known) for orientation only; they do not affect the calculated transition rates which assume only that the initial and final levels are good rotational states with good K values.

[b] Dipole (quadrupole) refers to pure $M1$ or $E1$ ($M2$ or $E2$) as demanded by the initial and final parities. For each initial level and final band one (the most intense measured) transition rate is normalized to unity for both experimental and theoretical entries. A theoretical entry of zero indicates a transition forbidden on spin-parity or K selection rule grounds. For greater perspective a number of experimental upper limits are given: These are obtained from the same data as the observed transitions but are, of course, not listed with the observed γ-ray lines of Table II. Experimental transition rates marked with an * refer to multiply placed lines and should be considered upper limits.

[c] γ-ray obscured by intense contaminant: no reasonable upper limit obtainable.

[d] Values not calculable since $L \geq K_i + K_f$.

would have $\Delta n_z = 2$, $\Delta\Sigma = 1$, and $\Delta\Lambda = 1$ hindrances. In addition, they would be slowed by a factor of ~10 relative to the observed deexcitation transitions by the $E_\gamma{}^3$ intensity dependence and considerably further reduced in intensity by the effects of pairing correlations.

The $\frac{1}{2}^-[501]$ band has also been located in ^{233}Th, ^{239}Pu, and ^{241}Pu and its γ decay has been studied.[6,7] In these nuclei the observed deexcitation routes are, as here, to the $\frac{1}{2}^+[631]$ band. Notable differences compared to ^{243}Pu are first, that in ^{239}Pu the γ-ray transition from the $\frac{3}{2}\frac{1}{2}^-[501]$ level to the $\frac{3}{2}\frac{1}{2}^+[631]$ level is weaker than those to the $\frac{1}{2}$ and $\frac{5}{2}$ members of the latter band whereas in ^{243}Pu all three transitions are comparable in strength and, secondly, in ^{233}Th this same initial state also deexcites strongly to the bandhead of the $\frac{5}{2}^+[622]$ orbital.

Turning now to transitions between even parity levels an interesting conclusion arises from comparison to the Alaga ratios. Most of the even parity levels can deexcite by a number of mixed $M1, E2$ transitions. For nearly all cases where the comparison can be made, agreement between experiment and the rotational model predictions for interband branching ratios is obtained if one assumes that the dominant multipolarity is $M1$ and not $E2$. A few examples are shown in Table IV. In only one case are the multipolarities actually measured, namely for the decay of the 287.4 keV level where $M1$ has been deduced[11] for the ground state transition. It is thus of some interest to calculate in detail the $M1$ and $E2$ transition rates to determine if, in fact, the former dominate. Thus, for each initial level we have calculated, in the framework of the Nilsson model, the $M1$ and $E2$ transition rates to all possible even parity final levels. The calculations were performed using a slightly modified form of the Coriolis coupling program CORCOUP written by Bunker and Starner.[20] The program allows for arbitrary attenuation of the Coriolis matrix elements including the limit of no mixing. Pairing was included with a gap parameter Δ of 0.75 MeV. The calculations incorporated the $\frac{7}{2}^+[624]$, $\frac{5}{2}^+[622]$, $\frac{1}{2}^+[631]$, $\frac{1}{2}^+[620]$, $\frac{3}{2}^+[622]$, and $\frac{3}{2}^+[631]$ Nilsson orbitals. All but the $\frac{3}{2}^+[622]$, and $\frac{1}{2}^+[620]$ were assigned as hole excitations. The initial states were those at 287.4, 333.2, 625.6, 654.0, 677.2, ~811, 845.4, and 981.1 keV. The $\frac{1}{2}^+[631]$ band members at 383.6, 392.3, and 447.0 keV must decay either by highly converted transitions to the 287.4 keV level or by K forbidden routes to the ground state band and are therefore not included.

Four sets of calculations were performed: with zero Coriolis mixing matrix elements for the cases $g_s = g_{s\,\text{free}}$, $g_R = 0.3$; $g_s = 0.6\, g_{s\,\text{free}}$, $g_R = 0.4$; $g_s = 0.6 g_{s_{\text{free}}}$, $g_R = 0.3$ and with unattenuated (attenuation factors $\equiv 1.0$) matrix elements for $g_s = g_{s_{\text{free}}}$, $g_R = 0.3$. Since we make no attempt as such to fit the data only one calculation with mixing was performed. It includes no free parameters and, with unity for all attenuation factors, most likely overemphasizes the effects of mixing. This is an adequate procedure in the present case because it will be seen that the calculated transition rates are quite insensitive to the mixing.

A comparison of some of the calculated transition rates with the data is given in Table V for the case of no mixing and $g_s = 0.6 g_{s_{\text{free}}}$ and $g_R = 0.3$. The most characteristic feature of all the calculations is the dominance of $M1$ over $E2$ multipolarities; expressed in transitions per second the difference is typically a factor of 10^3 or 10^4 in the absence of Coriolis mixing.

The second characteristic feature is that, as expected, the Coriolis mixing nearly always tends to significantly increase the $E2$ transition rates (typically by factors of 10^1–10^3) while leaving the $M1$ rates essentially unchanged. The reason is obvious, namely that the mixing of at least small amounts of each band into nearly all the others permits the $E2$ transitions to proceed essentially by large *intraband* transition rotational matrix elements. These intraband transition amplitudes are, of course, reduced by the mixing amplitudes (typically 0.03–0.15), but this is compensated by their *not* being reduced by the pairing correlations. Though the calculated $E2$ transition rates usually increase dramatically, the detailed extent of the change depends on the relative signs and magnitudes of the many possible intraband matrix elements involved. Even with the inclusion of Coriolis mixing, however, the $E2$ rates are still usually more than 10–100 times slower than the $M1$ rates, although in a few cases an $E2$ transition becomes as strong as 10–30% of the strongest $M1$ rate from the same initial level. It is also interesting that none of the four $E2$ rates that were large enough (>0.001 relative scale) to appear in Table V is increased by more than a factor of 10 by the Coriolis mixing. Thus the $M1/E2$ mixing ratios generally remain large. The earlier suggestion of $M1$ dominance, made on the basis of comparison of the data with the Alaga rules, thus is in accord with the detailed calculations. Since, furthermore, the $M1$ rates themselves seldom are affected by the mixing as much as a factor of 3, the overall effect of the Coriolis perturbation on the calculated transition rates is rather minor and it is not surprising that the Alaga rules satisfactorily accounted for many interband branching ratios. Of course, for detailed predictions of the relative strengths of transitions from each level to *different*

TABLE V. Comparison of measured relative γ-ray transition rates in ^{243}Pu with Nilsson model calculation.

Initial level		Final level		Relative transition rates [a]		
E (keV)	$JK^{\pi}[Nn_z\Lambda]$	E (keV)	$JK^{\pi}[Nn_z\Lambda]$	Theory [$M1$, ($E2$)]	Experiment	
287.4	$\frac{5}{2}\frac{5}{2}^+[622]$	0	$\frac{7}{2}\frac{7}{2}^+[624]$	1.0	1.0	
		58.1	$\frac{9}{2}\frac{7}{2}^+[624]$	F	0.018	
333.2	$\frac{7}{2}\frac{5}{2}^+[622]$	0	$\frac{7}{2}\frac{7}{2}^+[624]$	0.51	0.67	
		58.1	$\frac{9}{2}\frac{7}{2}^+[624]$	1.0	1.0	
		124	$\frac{11}{2}\frac{7}{2}^+[624]$	F	obsc.	
625.6	$\frac{1}{2}\frac{1}{2}^+[620]$	287.4	$\frac{5}{2}\frac{5}{2}^+[622]$	F	<0.06	
		333.2	$\frac{7}{2}\frac{5}{2}^+[622]$	F	<0.04	
		383.6	$\frac{1}{2}\frac{1}{2}^+[631]$	1.0	1.0	
		392.3	$\frac{3}{2}\frac{1}{2}^+[631]$	0.01	0.05	
		447.0	$\frac{5}{2}\frac{1}{2}^+[631]$	F	<0.05	
677.2	$\frac{5}{2}\frac{1}{2}^+[622]$	287.4	$\frac{5}{2}\frac{5}{2}^+[622]$	F	<0.12	
		333.2	$\frac{7}{2}\frac{5}{2}^+[622]$	F	1.4*	
		383.6	$\frac{1}{2}\frac{1}{2}^+[631]$	F	<0.14	
		392.3	$\frac{3}{2}\frac{1}{2}^+[631]$	1.0	1.0	
		447.0	$\frac{5}{2}\frac{1}{2}^+[631]$	0.54	obsc. (<0.9)	
See right hand column	$\frac{3}{2}\frac{3}{2}^+[622]$				809.6 keV	813.8 keV
		0	$\frac{7}{2}\frac{7}{2}^+[624]$	F, (0.38)	<0.06	0.96
		287.4	$\frac{5}{2}\frac{5}{2}^+[622]$	1.0	1.0	1.0
		333.2	$\frac{7}{2}\frac{5}{2}^+[622]$	F	<0.2	0.32
		383.6	$\frac{1}{2}\frac{1}{2}^+[631]$	0.15	0.28	<0.04
		392.3	$\frac{3}{2}\frac{1}{2}^+[631]$	0.12	obsc.	<0.06
		447.0	$\frac{5}{2}\frac{1}{2}^+[631]$	0.02	<0.09	<0.03
		625.6	$\frac{1}{2}\frac{1}{2}^+[620]$	0.07	<0.4	<0.10
		654.0	$\frac{3}{2}\frac{1}{2}^+[620]$	0.03	obsc.	0.30
		677.2	$\frac{5}{2}\frac{1}{2}^+[620]$	0.005	obsc.	obsc.
981.1	$\frac{5}{2}\frac{3}{2}^+[631]$	0	$\frac{7}{2}\frac{7}{2}^+[624]$	F	<0.41	
		58.1	$\frac{9}{2}\frac{7}{2}^+[624]$	F	<0.14	
		287.4	$\frac{5}{2}\frac{5}{2}^+[622]$	0.49, (0.02)	0.32	
		333.2	$\frac{7}{2}\frac{5}{2}^+[622]$	1.0	0.43*	
		383.6	$\frac{1}{2}\frac{1}{2}^+[631]$	F	<0.61	
		392.3	$\frac{3}{2}\frac{1}{2}^+[631]$	0.038, (0.004)	1.0	
		447.0	$\frac{5}{2}\frac{1}{2}^+[631]$	0.032, (0.004)	0.80	

TABLE V *(Continued)*

Initial		Final level		Relative transition rates [a]	
E(keV)	$JK^{\pi}[Nn_z\Lambda]$	E(keV)	$JK^{\pi}[Nn_z\Lambda]$	Theory [$M1$, ($E2$)]	Experiment
981.1	$\frac{5}{2}\frac{3}{2}^+$ [631]	625.6	$\frac{1}{2}\frac{1}{2}^+$ [620]	F	<0.14
		654.0	$\frac{3}{2}\frac{1}{2}^+$ [620]	<0.001	<0.49
		677.2	$\frac{5}{2}\frac{1}{2}^+$ [620]	<0.001	<0.30
		813.8	$\frac{3}{2}\frac{3}{2}^+$ [622]	<0.001	obsc.

[a] The theoretical entries are calculated $M1$ and $E2$ transition rates obtained using the listed Nilsson assignments with the Nilsson model parameters $\mu=0.325$, $\kappa=0.0635$, and with $g_s=0.6\,g_{s_{\text{free}}}$ and $g_R=0.3$. Coriolis mixing was not included. See text for discussion of the effects of using different g_s and g_R values, and of including Coriolis mixing. The format for the theoretical entries is as follows: For each initial level the strongest transition is normalized to 1.0. Numbers standing alone are $M1$ transition rates and an F indicates that the $M1$ transition is spin or K forbidden. Numbers in parentheses are $E2$ transition rates in the same units as the $M1$ entries; they are omitted if less than 0.001, and no indication of forbiddenness is included. Thus for only four levels are $E2$ rates larger than 0.1% of the strongest calculated $M1$ transition from the same initial level, and in those cases where the $M1$ transition is not forbidden the $E2$ rate is $\lesssim\frac{1}{10}$ the $M1$ rate. As discussed in the text, the Coriolis mixing usually increases the $E2$ rate but of those large enough to be included in this table none is increased except for the 981.1-287.4 keV transition whose $E2$ rate becomes ~0.15 in the units of this table. The experimental entries are separately normalized to 1.0 for the strongest observed transition from each level. The entry "obsc." indicates a transition which is either obscured or which has an energy below our cutoff. For the $\frac{3}{2}\frac{3}{2}^+$[622] level the experimental entries are tabulated for the two choices for the level assignment. The experimental entries for the 809.6 keV state assume that all of the intensity of the doubly placed transitions stem from this level. In other cases the symbol * refers to multiply placed lines whose intensities should be considered upper limits: the symbol < denotes experimental upper limits on *unobserved* transitions. Tentatively placed transition are entered with their full intensity for the purposes of the table.

intrinsic final states, the full Nilsson calculation is necessary.

The changes in $M1$ rates due to substituting $g_s=g_{s_{\text{free}}}$ for $g_s=0.6g_{s_{\text{free}}}$ are in many cases more significant than those from Coriolis mixing and any sizable uncertainty in the effective g_s (or even in g_R) probably has comparable influence on the predictions as does the Coriolis force. Of course, for the cases where $L<K_i+K_f$, changes in g_s and g_R do not affect the relative $M1$ transition intensities to a given final band. With the above caveats in mind, it should be clear that Table V should be scanned only to identify the major calculated and experimental deexcitation modes for each initial level.

The deexcitation of the $\frac{5}{2}^+$[622] orbital must go to the $\frac{7}{2}^+$[624] band. The calculations only serve to predict the $M1$ dominance and therefore the Alaga ratios for dipole transitions.

For the $\frac{1}{2}^+$[620] band, the table shows reasonable agreement between the calculated and observed transitions out of the 625.6 and 677.2 keV states, although a large intensity of the multiply placed 343.9 keV transition (677.2→333.2 keV) is not predicted, even by the calculations including Coriolis mixing. For the level at 654.0 keV, the strongest transition on theoretical grounds would be obscured, so we present no further comparison except to note that the γ-ray feeding the 392.3 keV level is also predicted to be very intense.

The $\frac{3}{2}\frac{3}{2}^+$[622] state observed in the (d,p) reaction near 810 keV has been associated above with either the 809.6 or 813.8 keV level from the (n,γ) experiments. The present calculations do not resolve the question since both levels are characterized, in agreement with the calculations, by strong transitions to the 287.4 keV level and yet both also have decay patterns at variance with the calculations (e.g., no ground state decay for the 809.6 keV level and transitions to the 333.2 and 654.0 keV levels for the 813.8 keV state). The same initial state in ^{235}U depopulates to the $\frac{5}{2}\frac{5}{2}^+$[622] level but not the $\frac{7}{2}\frac{7}{2}^+$[624] state.[5] It feeds the $\frac{1}{2}^+$[631] band fairly strongly as well. In ^{241}Pu the $\frac{3}{2}\frac{3}{2}^+$[622] level at 942.5 keV is observed[6] to deexcite only to the $\frac{1}{2}^+$[631] band. These comparisons would favor the association of the state seen in the (d,p) reaction with the 809.6 keV level.

The next rotational state of the $\frac{3}{2}^+$[622] band in ^{243}Pu is at 845.4 keV and is characterized both

theoretically and experimentally by transitions to the $\frac{7}{2}^+[624]$ and $\frac{5}{2}^+[622]$ bands. Further analysis is pointless, though, since the strongest calculated transition has $E_\gamma = 512.2$ keV and is obscured by annihilation radiation.

Finally, the calculations for the $\frac{5}{2}^+$ member of the $\frac{3}{2}^+[631]$ band at 981.1 keV account for the strong transitions to the $\frac{5}{2}^+[622]$ band but do not explain the strengths of those to the $\frac{1}{2}^+[631]$ band members at 392.3 and 447.0 keV. However, if $g_s = g_{s\,\text{free}}$ the calculated intensities of these two transitions increase relative to those to the $\frac{5}{2}^+[622]$ band by a factor of ~50; such a parameter change would produce rather good agreement with the data. In any case, the empirical preference for depopulation to the $\frac{5}{2}^+[622]$ and $\frac{1}{2}^+[631]$ bands rather than to the $\frac{7}{2}^+[624]$ and $\frac{1}{2}^+[620]$ bands is correctly calculated. The decay of this same band in ^{235}U and ^{233}Th is similar[5,7] with most of the intensity feeding the $\frac{1}{2}^+[631]$ band and weak transitions terminating in the $\frac{5}{2}^+[622]$ band.

To summarize these results, the general pattern of deexcitation, that is the general preferences for decay to specific lower-lying Nilsson orbits rather than to others, is well reproduced by the above calculations. A few significant discrepancies remain, however, for individual transitions, and further theoretical treatment is needed.

B. Differences in the residual interaction between $K^\pi = \frac{1}{2}^-$ bands in ^{243}Pu and ^{241}Pu

Unlike the case of ^{241}Pu,[2] we do not observe any mixing of the $\frac{1}{2}^-[501]$ and $\frac{1}{2}^-[750]$ states in ^{243}Pu. This is especially puzzling since in ^{243}Pu and ^{241}Pu the states have similar excitation energies. Their energies differ from each other by about 135 keV in ^{241}Pu and by 115 keV in ^{243}Pu; yet in ^{241}Pu the lower $K^\pi = \frac{1}{2}^-$ band appears to be a 50% mixture of each of the two states. The only major difference between the two nuclei is the shift in the Fermi surface from the vicinity of the $\frac{5}{2}^+[622]$ orbital in ^{241}Pu to the vicinity of the $\frac{7}{2}^+[624]$ orbital in ^{243}Pu and also the blocking of these orbitals by the odd nucleon in their respective nuclei. It has been suggested by Chasman[21] that it is an interaction with a nonsingle particle $K^\pi = \frac{1}{2}^-$ state which is responsible for the mixing in ^{241}Pu. This implies that in ^{243}Pu this "third" state has changed in energy or character and no longer interacts strongly. Proof of this hypothesis can only be obtained by use of ultrahigh-resolution spectroscopy to identify the "third" state in both nuclei. Experiments of this kind have recently become feasible due to the increased energy stability of the Argonne tandem Van de Graaff accelerator and are in preparation.

---

*Work supported by the U.S. Energy Research and Development Administration.

† Permanent address: East Texas State University, Commerce, Texas 75428.

[1] T. H. Braid, R. R. Chasman, J. R. Erskine, and A. M. Friedman, Phys. Rev. C 1, 275 (1970).

[2] T. H. Braid, R. R. Chasman, J. R. Erskine, and A. M. Friedman, Phys. Rev. C 6, 1374 (1972).

[3] T. H. Braid, R. R. Chasman, J. R. Erskine, and A. M. Friedman, Phys. Rev. C 4, 247 (1971).

[4] S. Bjørnholm, J. Dubois, and B. Elbek, Nucl. Phys. A118, 241 (1968).

[5] F. A. Rickey, E. T. Jurney, and H. C. Britt, Phys. Rev. C 5, 2072 (1972).

[6] P. Matussek, in *Proceedings of the Second International Symposium on Neutron Capture Gamma Ray Spectroscopy and Related Topics, Sept. 2–6, 1974, Petten, the Netherlands* (Reactor Centrum Nederland, Petten, 1975), p. 655.

[7] T. von Egidy, O. W. B. Schult, D. Rabenstein, J. R. Erskine, O. A. Wasson, R. E. Chrien, D. Breitig, R. P. Sharma, H. A. Baader, and H. R. Koch, Phys. Rev. C 6, 266 (1972).

[8] W. Teoh, R. D. Connor, and R. H. Betts, Nucl. Phys. A228, 432 (1974).

[9] *Resonance Parameters,* compiled by S. F. Mughabghab and D. I. Garber, Brookhaven National Laboratory Report No. BNL-325 (National Technical Information Service, Springfield, Virginia, 1973), 3rd ed., Vol. 1.

[10] W. R. Kane, D. Gardner, T. Brown, A. Kevey, E. der Mateosian, G. T. Emery, W. Gelletly, M. A. T. Mariscotti, and I. Schröder, *Proceedings of the International Symposium on Neutron Capture Gamma Ray Spectroscopy, Studsvick, Sweden, 11–15 August, 1969* (International Atomic Energy Agency, Vienna, 1969), p. 105.

[11] P. R. Fields, I. Ahmad, A. M. Friedman, J. Lerner, and D. N. Metta, Nucl. Phys. A160, 460 (1971).

[12] S. W. Yates, I. Ahmad, A. M. Friedman, F. J. Lynch, and R. E. Holland, Phys. Rev. C 11, 599 (1975).

[13] J. E. Spencer and H. A. Enge, Nucl. Instrum. Methods 49, 181 (1967).

[14] J. R. Erskine and R. H. Vonderohe, Nucl. Instrum. Methods 81, 221 (1970).

[15] N. Williams (private communication).

[16] A. H. Wapstra, K. Bos, and H. B. Gove, 1974 Supplement to 1971 Atomic Mass Adjustment Tables, Nucl. Data A9, 265 (1971), private communication.

[17] K. Neergaard and P. Vogel, Nucl. Phys. A149, 217 (1970).

[18] G. Alaga, K. Alder, A. Bohr, and B. R. Mottelson, K. Danske Vidensk. Selsk. Mat. Fys.–Medd. 29, no. 9 (1955).

[19] O. Nathan and S. G. Nilsson, *Alpha-, Beta-, and Gamma Ray Spectroscopy,* edited by K. Siegbahn (North-Holland, Amsterdam, 1965).

[20] J. W. Starner and M. E. Bunker, code CORCOUP.

[21] R. R. Chasman (private communication). We wish to thank Dr. Chasman for allowing us to quote these results while his calculations are still at a preliminary stage.